International Journal of Pharmaceutics 414 (2011) 218–224

Contents lists available at ScienceDirect

International Journal of Pharmaceutics

journal homepage: www.elsevier.com/locate/ijpharm

An investigation into silk fibroin conformation in composite materials intended for drug delivery

Francesco Cilurzo*, Chiara G.M. Gennari, Francesca Selmin, Laura A. Marotta, Paola Minghetti, Luisa Montanari

Department of Pharmaceutical Sciences "Pietro Pratesi", Università degli Studi di Milano, Via G. Colombo, 71 – 20133 Milan, Italy

ARTICLE INFO

Article history:
Received 24 February 2011
Received in revised form 28 April 2011
Accepted 5 May 2011
Available online 12 May 2011

Keywords:
Silk fibroin
Spray-drying
Casting
ATR-FTIR spectroscopy

ABSTRACT

Regenerated silk fibroin (SF) is a promising biomaterial to design drug delivery systems. To guarantee satisfactory prolonged release of loaded drugs, the native β-sheet conformation of SF is generally induced by a final curing which can determine instability of the loaded drug. This work aimed to investigate the influence on SF conformation of the addition of hydrophilic polymers, namely poloxamer 188 (PEO), a range of poly(ethylenglycol) (PEG)and poly(vinyl pyrrolidone) (PVP) and drying conditions, namely spray-drying or evaporation at 60 °C. DSC data on spray-dried products indicated that SF in composite materials was in the random coil conformation. ATR-FTIR spectroscopy with Fourier self-deconvolution of the amide I band revealed that SF in spray dried products was partially organized in the β-sheet structure only in presence of PEG4000.

Both DSC and ATR-FTIR spectra registered on composite materials obtained by the slowest evaporation method indicated that all hydrophilic polymers favoured the β-sheet conformation. This feature was attributed to the formation of H-bonds with the tyrosine residues of the semicrystalline region in SF. In conclusion, this approach to prepare of SF/hydrophilic polymer composites at slow evaporation rate leads to water insoluble materials which could be used in the development of drug delivery systems.

1. Introduction

Silk fibroin, a naturally occurring protein spun by the silkworm *Bombyx mori*, is a promising biomaterial for the incorporation and delivery of a range of therapeutic agents due to its unique properties such as slow biodegradation, good mechanical properties, and favourable processability in combination with biocompatibility (Vepari and Kaplan, 2007; Numata and Kaplan, 2010).

Several drug delivery constructs with different morphologies such as films (Hofmann et al., 2006), microspheres (Wang et al., 2007, 2008), nanoparticles (Kundu et al., 2010) and hydrogels (Numata and Kaplan, 2010), have been proposed to control the release of both small molecule drugs and proteins, such as enzymes and cell growth factors.

Natural silkworm silk fibres form predominantly crystalline β-sheet structures leading to stability, long-time degradability and the unique mechanical resistance (Cao and Wang, 2009). However, in order to prepare drug delivery systems, it is necessary to dissolve silk fibres in a solvent capable of denaturing the fibroin by breaking the strong intermolecular hydrogen bonds (Kaplan et al., 1997). Once the silk protein is dissolved, it can be processed into a variety of different material morphologies by different processes. Afterwards, a final curing is often required to enrich regenerated silk fibroin (SF) in β-sheet structure and, thus, induce water insolubility. This particular structure of SF is generally controlled by stretching, compression, annealing and/or chemical treatment in order to tune-up mechanical and degradability properties of films (Minoura et al., 2009). Additionally, the correlation between conformation of SF and drug release was also reported (Hofmann et al., 2006): the higher the crystalline content of SF, the slower the release of the encapsulated proteins. The ability to regulate the structure and morphology of SF in an all-aqueous process and/or mild processing technologies renders this biomaterial an important candidate for drug delivery applications. Furthermore, the use of final curing should be minimized, or even circumvented in order to incorporate efficaciously sensitive biologics and reduce detrimental and/or toxic effects of residual solvents (Sashina et al., 2006).

To overcome these drawbacks, the blending of SF with natural or synthetic polymers (Hardy and Scheibel, 2010) has also considered since SF and the auxiliary material might mutually aggregate to form a new ordered structure, which may guarantee the required mechanical strength as well as water insolubility avoiding post-treatment. In particular, the mechanical properties of regenerated SF fibroin have been improved by mixing with poly(ethylene glycol) 400 (PEG 400) (Wang et al., 2003).

* Corresponding author. Tel.: +39 02 503 24635; fax: +39 02 503 24657.
E-mail address: francesco.cilurzo@unimi.it (F. Cilurzo).

0378-5173/$ – see front matter © 2011 Published by Elsevier B.V.
doi:10.1016/j.ijpharm.2011.05.023

The purpose of the present study is to expand the understanding of the effects of blending SF with other hydrosoluble polymers and drying conditions on the conformation of the dried SF. With this aim, composite materials based on SF and poloxamer (PEO), poly(vinyl pyrrolidone) (PVP) or an homologue series of poly(ethylene glycol) (PEG) were prepared by spray-drying or casting methods. These evaporation conditions were selected in order to evaluate also the effect of the evaporation rate other than the composition of the composite material on the SF conformation.

2. Materials and methods

2.1. Materials

Lutrol® F 68 (Poloxamer 188, PEO, M_w = 8600 Da) and Kollidon® K30 (poly(vinyl pyrrolidone), PVP) were kindly gifted by BASF (Germany). Poly(ethylene glycol) 4000 (PEG4000; hydroxyl value = 26–32 mg KOH/g; M_w = 3600–4400 Da) and poly(ethylene glycol) 600 (PEG600; hydroxyl value = 170–208 mg KOH/g; M_w = 540–660 Da) were provided by Polichimica (Italy), poly(ethylene glycol) 1000 (PEG1000; hydroxyl value = 102–125 mg KOH/g; M_w = 900–1100 Da) and poly(ethylene glycol) 1500 (PEG1500; hydroxyl value = 68–83 mg KOH/g; M_w = 1350–1650 Da) were purchased from Sigma–Aldrich (Italy).

2.2. Preparation of regenerated fibroin solution

Regenerated fibroin solutions (SF) were obtained by degumming raw *B. mori* silk and dissolving the degummed silk fibres (about 7.2 g) in 100 mL $CaCl_2$ hydroalcoholic solution ($CaCl_2/H_2O$/EtOH, mole ratio 1:8:2) at 70 °C for 2 h and shaken at 200 rpm in a thermostated bath. The regenerated fibroin was dialyzed in a cellulose tube (MWCO 12,000 Da, Sigma–Aldrich, Italy) against distilled water for 3 days at room temperature to remove salts and ethanol. The final solution was filtered with a metallic strainer and, then, centrifuged for 20 min at 5000 rpm to eliminate the precipitated fibroin. The final fibroin solution concentration was about 3.2% (w/w), determined by weighting the remaining solid after drying.

2.3. Drying process

Spray drying: The feed was obtained by blending the fibroin solution and the selected polymer, namely PEO, PVP, PEG1000 and PEG4000, in the 95/5% (w/w) ratio. The feed was sprayed through a standard nozzle with inner diameter of 0.6 mm (Lab-Plant model SD04, UK). Process parameters: inlet temperature 130 °C; outlet temperature 85 °C; feed flow rate 11 mL/min. The pure regenerated SF was spray dried according to the same procedure.

Casting method: The selected polymer, namely PEO, PVP and PEG1000, were added to 3.2% (w/w) SF solution in the ratio 5/95% (w/w) and gently stirred at room temperature to homogeneously disperse. Afterwards, the solution was casted on the bottom of a polystyrene Petri dish and dried in an oven thermostated at 60 °C until constant weight. The cast material made only by the regenerated SF was also prepared according to the same protocol.

The effects of PEG molecular weight and SF/PEG ratio on the molecular conformation of SF were investigated. Films at PEG/SF ratio ranging from 99/1 to 60/40% (w/w) were prepared by using PEG600, PEG1000, PEG1500 and PEG4000.

2.4. Scanning electron microscopy

The surface morphology and shape of the spray-drying materials were analyzed by SEM (JSM-T 800-JEOL, I). The samples were sputtered with an Au/Pd coating in an argon atmosphere.

2.5. Thermal analysis

DSC data were recorded by using a DSC 2010 TA (TA Instruments, USA). The samples were sealed in aluminium pans and heated in inert atmosphere (70 mL/min N_2) at 20 K/min from 30 to 350 °C. The reference was an empty pan. The equipment was calibrated with an indium sample. All measurements were performed in duplicate. The residual water content in the SF and SF/polymer materials was determined by thermogravimetric analyses using a TGA 2050 thermogravimetrical analyzer (TA Instruments, USA). Samples of approximately 20 mg were heated in a platinum crucible at 5 K/min under a nitrogen atmosphere and the loss of weight was recorded.

2.6. Attenuated total reflection Fourier transform infrared spectroscopy (ATR-FTIR)

FTIR measurements were performed using a Spectrum™One spectrophotometer (PerkinElmer, USA), by placing the samples on a diamond crystal mounted in ATR cell (PerkinElmer, USA). The spectra recorded at 2 cm^{-1} resolution and 32 scans were collected over the wavenumber region 4000–650 cm^{-1}. The analyses were performed on raw polymers and on spray-dried and cast materials. To assess the homogeneity in composition, FTIR spectra were recorded at least in three different points of the cast materials.

Fourier self-deconvolution (FSD) of the overlapping amide I band components (1585–1700 cm^{-1}) was made possible by using Peakfit 4.12 software (Galactic Industries Corporation, New Hampshire, USA). Spectra were baseline corrected, smoothed with a nine-point Savitsky–Golay function (Savitzky and Golay, 1964). The amide I bands were resolved by the second-order derivative with respect to the wavelength. Deconvolution was performed using Gaussian line shape with an amplitude threshold of 3%. A nonlinear least-square method was finally used to take the reconstituted curve as close as possible to the original deconvoluted spectra. The fitting results were further evaluated by examining the residual from the differences between the fitted curve and the original curve.

3. Results and discussion

3.1. Effect of drying conditions

Depending on the processing conditions, regenerated SF can preferentially assume random coil and β-sheet conformation (Hino et al., 2003; Li et al., 2001). ATR-FTIR spectroscopy with Fourier self-deconvolution and DSC analysis are useful tools to investigate and quantify both contributions to the molecular conformations of this protein.

The main differences reside in the position of absorption bands of amide I, amide II and amide III reflecting the different ratio between intra- and inter-molecular hydrogen bonds. In agreement with literature data, the degummed SF presented the characteristic β-sheet conformation (Boudet-Audet et al., 2008) and the absorption bands of amide I, amide II and amide III were centred at 1620 cm^{-1}, 1511 cm^{-1} and 1227 cm^{-1}, respectively (Fig. 1). In the same spectrum, two shoulders on the amide I and amide III bands were detected at 1696 cm^{-1} and 1265 cm^{-1}, respectively. In the ATR-FTIR spectrum of the spray-dried SF, the amide bands (amide I: 1638 cm^{-1}; amide II: 1515 cm^{-1} and amide III:

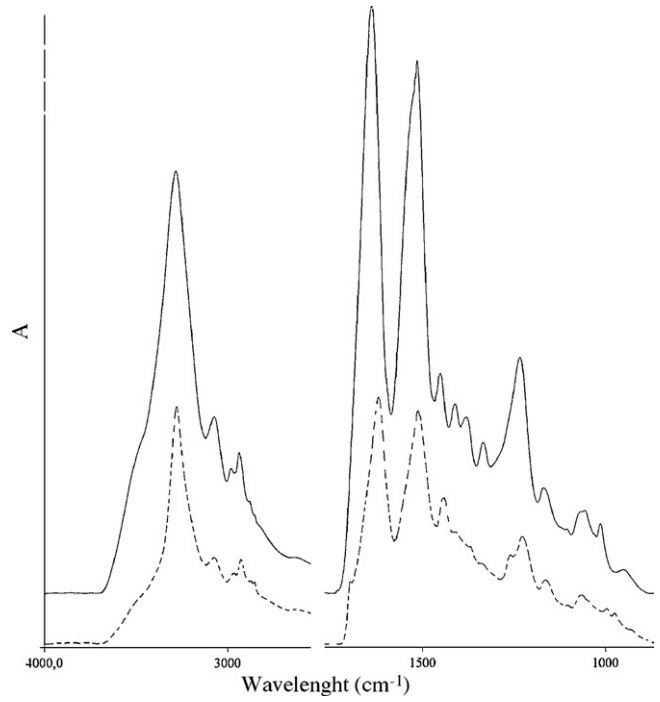

Fig. 1. ATR-FTIR spectra of the degummed (dash line) and spray-dried SF (solid line).

1233 cm^{-1}) were recorded at higher wavelengths and the shoulders on the amide I and the amide III were not detectable (Fig. 1). These features were due to a prevalent random coil conformation (Taddei and Monti, 2005). The spectrum of the cast SF was very close to that of the spray-dried SF, even if the bands assigned to amide I (1635 cm^{-1}), and amide III (1231 cm^{-1}) slightly shifted towards higher wavenumbers, suggesting the formation of a less disordered structure in the cast SF.

DSC data confirmed the difference in spatial organization of the degummed SF, spray-dried and cast SF. The former pattern evidenced only the peak at about 300 °C attributed to thermal decomposition of the crystalline material after the endothermic event related to water evaporation at about 100 °C (Fig. 2). The DSC profile of spray-dried SF showed the glass transition temperature at 179 °C, typical of the random coil conformation, followed by an exothermic peak at 218 °C (23 J/g) attributed to the transition from random coil to β-sheet structure, and the thermal decomposition of the material at 299 °C (Fig. 2). As expected, the thermal parameters of cast SF were superimposable to spray-dried SF (data not shown). The residual water content in the tested samples determined by a thermogravimetric method was about 7.5–10% (w/w).

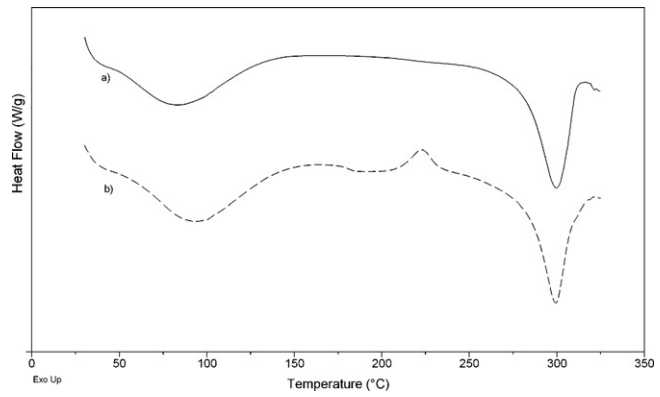

Fig. 2. DSC data of the degummed (a, solid line) and spray-dried SF (b, dash line).

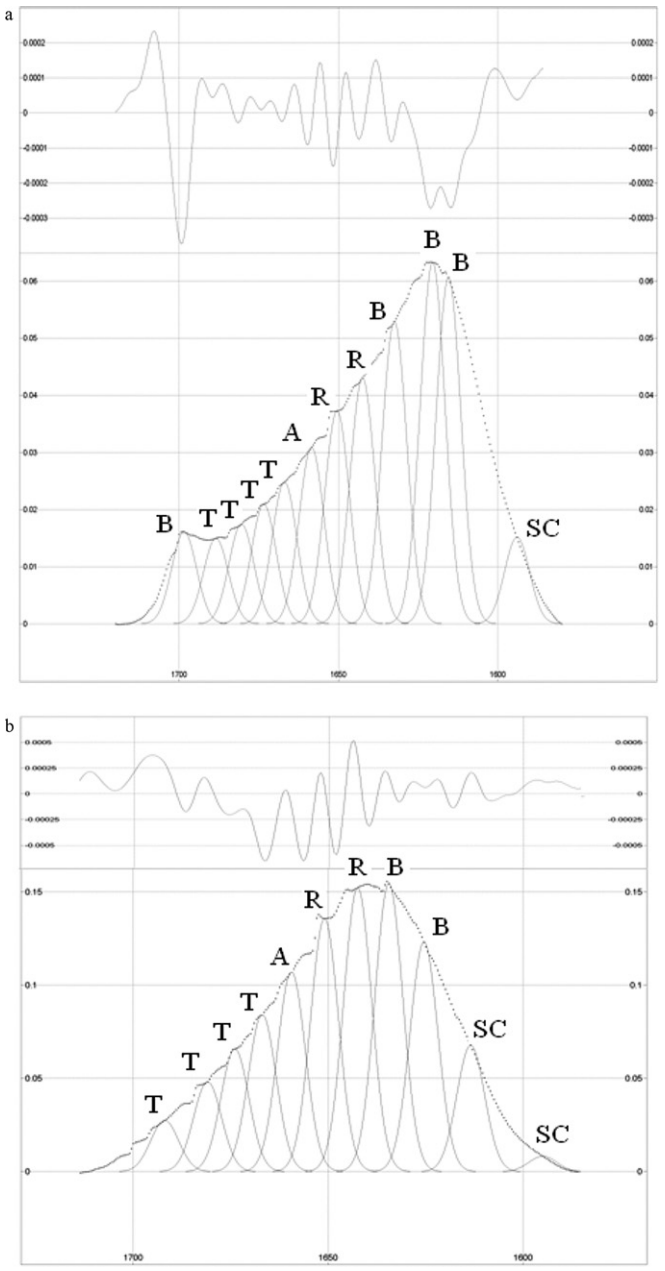

Fig. 3. Absorbance spectra in the amide I region, deducted after Fourier transform self-deconvolution of (a) degummed and (b) spray-dried SF. The solid and dotted curves represent the original and the fitted spectra, respectively. The attributions of each deconvoluted band are marked as R (random coil), B (β-sheets), A (α-helices), T (turns), and SC (side chains). In the upper part of the graphs, the second derivative of the original spectrum was reported.

A deeper insight on the molecular conformation of SF dried according to the different procedures was carried out by Fourier self-deconvolution (FSD) of amide I region of the relative ATR-FTIR spectra. The deconvolution permitted to identify 11 peaks and the fitting revealed a good sound of correlation ($r^2 > 0.97$). Fig. 3a and b reports Gaussian curve fitting of the amide I region for the degummed and spray-dried SF, respectively. The amide I region bands were assigned to the different conformation of SF with reference to the literature (Hu et al., 2006). The band centred at about 1633 cm^{-1} was attributed to intramolecular β-sheet (B); the peak at 1699 cm^{-1} and the bands in the1613–1625 cm^{-1} region are due to intermolecular β-sheets (B). In the region between 1667 and 1694 cm^{-1}, three or four peaks were found and assigned to the

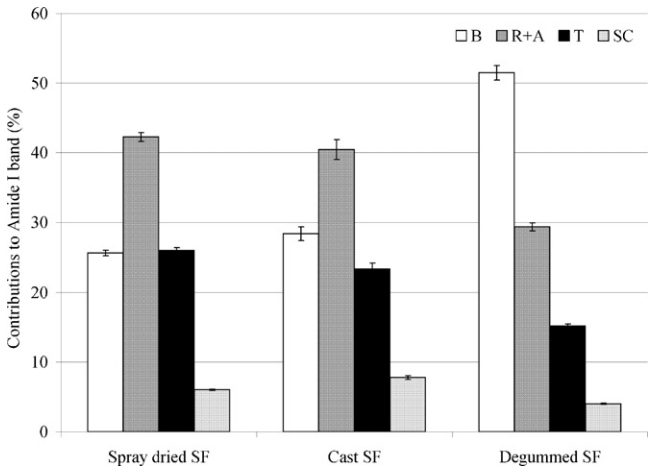

Fig. 4. Contributions to the ATF-FTIR amide I band determined by Fourier transform self-deconvolution for regenerated SF as a function of the drying condition. Degummed SF was selected as control of crystallized sample. Each data point represents the percentage of the peak areas attributed to: β-sheets (B); random coils and α-helices (R + A); turns (T); side chains (SC). The coefficient of variation of these data lower was than 3.5 ($n = 2$).

turn structure (T), which represents the less ordered crystalline structure (Hu et al., 2006). The contribution of the random coil (RC) conformation was represented by two peaks centred at about 1642 and 1651 cm^{-1}. The band assigned to the α-helices (A) was centred at 1659–1660 cm^{-1}. The absorption peaks related to the side chains or aggregated strands (SC) were detected in the 1595–1613 cm^{-1} region. The main difference in the deconvoluted amide I band of the degummed SF and spray dried product resides in the number of peaks assigned to the β-sheets. In particular, three intense bands assigned in the region from 1617 to 1637 cm^{-1} were found in the degummed SF and the weak β-sheet band at 1699 cm^{-1} was not detected in the spray-dried product. A further difference in the two deconvoluted spectra consists in the number of peaks attributed to the turns structure (Fig. 3a and b). The pattern of the cast SF was ascribed to the spray dried product.

In order to better evidence the differences of SF spatial organization following different drying procedures, the relative amounts of the secondary structural elements were quantified by summing the area of peaks with the same attribution and the data were normalized with respect to the total amide I area (Fig. 4). In both dried samples, the β-sheet fraction significantly decreased in parallel with the increase of the random coil/α-helices contribution with respect to the degummed SF. These events appear remarkable in the spray-dried sample, confirming that the faster the evaporation, the lower the ability of fibroin molecules to form an ordinate structure.

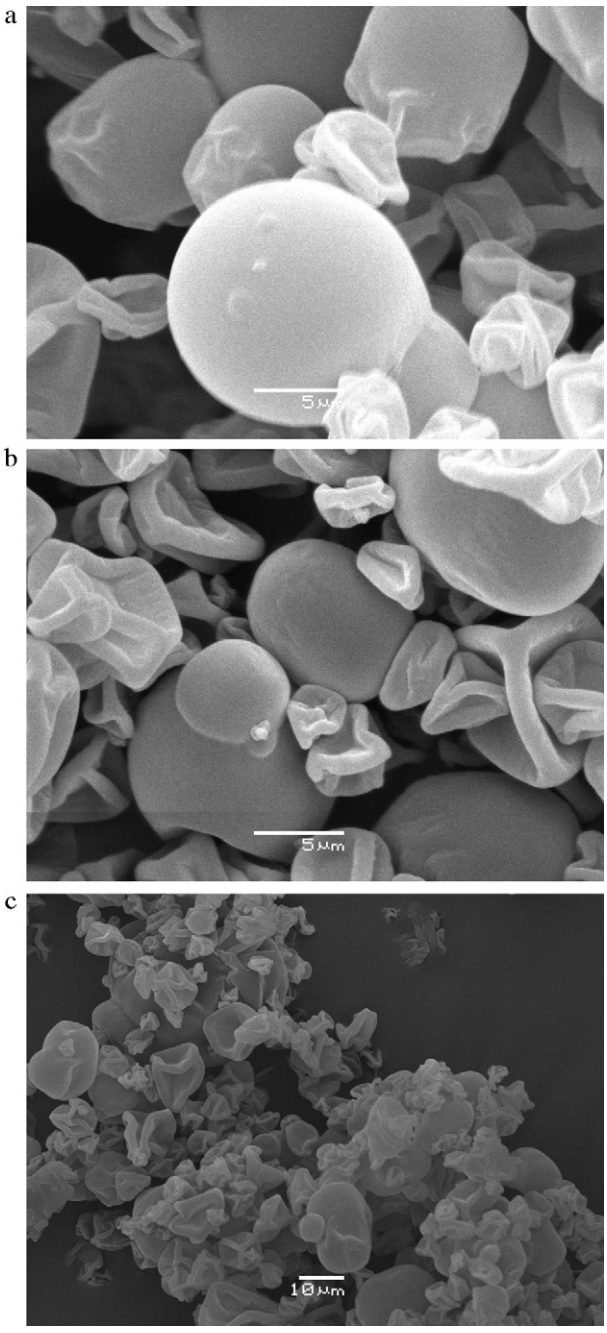

Fig. 5. SEM microphotography of spray dried products made of (a) SF/PVP; (b) SF/PEO and (c) SF/PEG.

3.2. Effect of the blending

The blending of SF to an auxiliary material is considered a suitable approach to induce the transition of SF from random coil to β-sheets (Hardy and Scheibel, 2010). After mixing SF to PEO, PVP, PEG1000 and PEG4000 at the ratio of 5/95% (w/w), the solutions were dried by spray-drying or casting.

The morphology of spray-dried blends appeared irregular (raisin-like structure) with a smooth surface. In the microphotographs no signs of dishomogeneity were evident independently of the nature of blended polymer (Fig. 5a–c). The four materials obtained by casting procedure appeared smooth and transparent (data not shown).

The spectra of spray-drying blends showed significant differences with respect to the degummed SF (Fig. 6). Of particular interest is the amide III region since it allowed the discrimination among spray-dried blends. Indeed, the shoulders on amide I and amide III at about 1263 cm^{-1} attributed to the β-sheet conformation of SF (Hino et al., 2003) was detected only in presence of PEG4000. The analysis of deconvoluted amide I band confirmed these data. The amide I region of the spray-dried product made of SF/PVP was not resolved because of an interference of the PVP stretching band detected at about 1645 cm^{-1}. The calculated contribution to β-sheets was in 24–26% for spray-dried SF/PVP, SF/PEO, and SF/PEG1000 products indicating that such materials were not effective to induce the transition towards an ordered structure since the calculated contribution to β-sheets were not statistically different from the spray-dried SF (one-way ANOVA, $p = 0.57$). In the case of spray-dried SF/PEG4000 the contribution to β-sheets

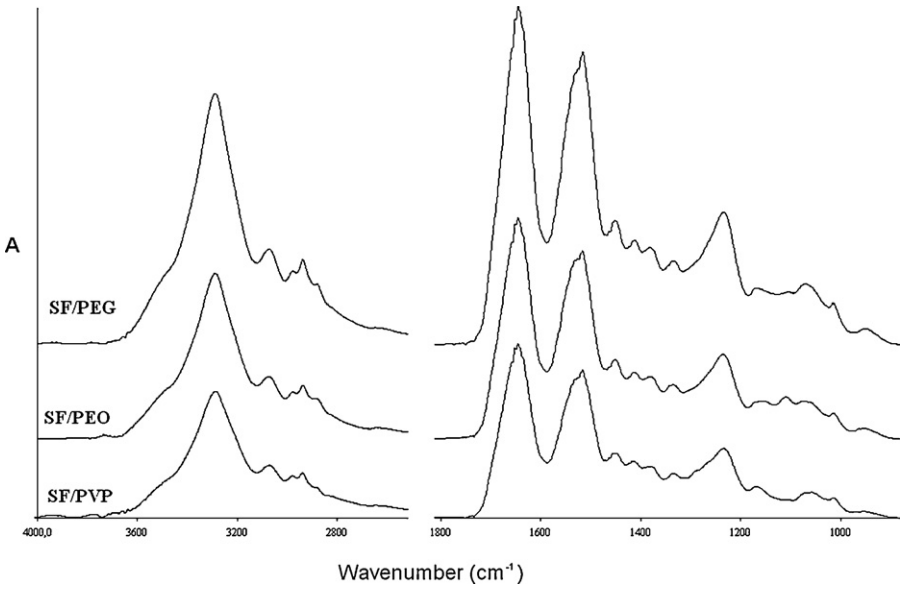

Fig. 6. ATR-FTIR spectra of spray-drying products.

Table 1
DSC data of spray-dried SF and blends at the ratio 95/5 (%, w/w).

	T_g (°C)	Transition α → β			Degradation
		T_{onset} (°C)	T_{max} (°C)	ΔH (J/g)	T_{max} (°C)
Spray-dried SF	181.0 ± 1.1	211.6 ± 0.3	220.7 ± 0.7	23.08 ± 1.3	299.4 ± 0.3
SF/PVP	182.2 ± 0.9	213.8 ± 0.7	225.2 ± 0.4	29.2 ± 1.5	295.4 ± 0.1
SF/PEO	181.7 ± 1.4	209.1 ± 0.4	221.2 ± 0.3	32.3 ± 1.4	296.6 ± 0.1
SF/PEG1000	179.7 ± 1.1	204.3 ± 0.3	219.3 ± 0.6	23.8 ± 1.4	296.7 ± 0.2
SF/PEG4000	181.0 ± 1.3	201.1 ± 0.2	219.5 ± 0.3	16.2 ± 0.9	299.0 ± 0.2

resulted about 30% ($p < 0.01$). This partial conversion of SF to the crystalline structure after the rapid evaporation of the feed evidenced the key role played by the PEG average molecular weight.

DSC results of spray-dried products indicated the typical thermal behaviours of the random coil structure. The glass transition temperature (T_g) was detected at about 180 °C independently of the blended polymers (Table 1). In presence of PVP, PEO and PEG1000, the transition from random coil to β-sheets occurred at temperature comparable to that measured for the spray-dried SF. The same transition in the SF/PEG4000 blend was recorded at higher

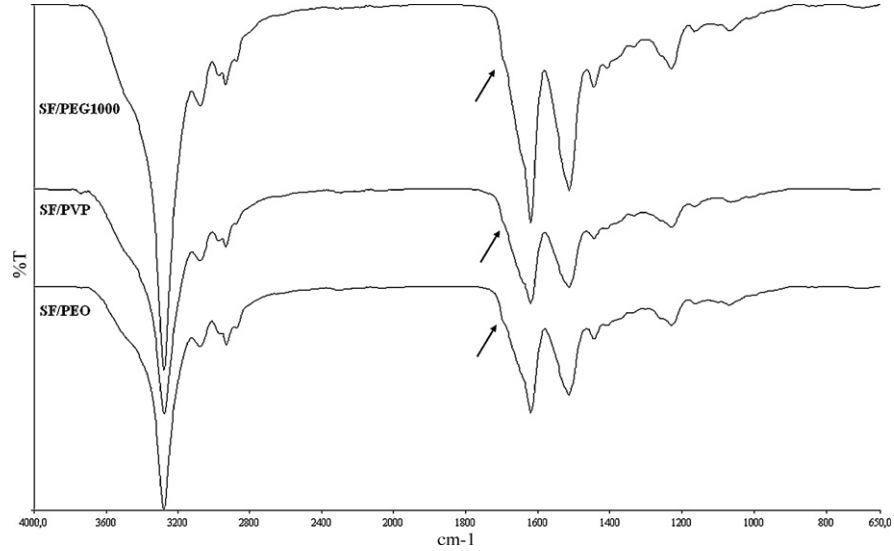

Fig. 7. ATR-FTIR spectra of films prepared by blending the regenerated SF with PEO, PVP and PEG 1000 at 95/5% (w/w) ratio.

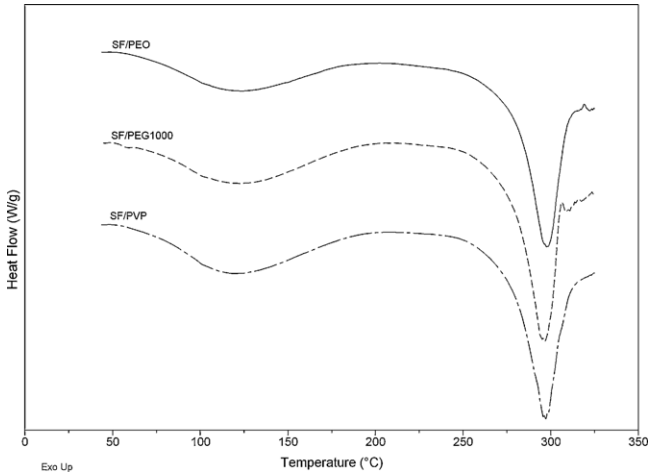

Fig. 8. DSC data on films prepared by blending the regenerated SF with PEO (solid line), PVP (broken dash line) and PEG 1000 (dash line) at 95/5% (w/w) ratio.

temperatures with an increase in the enthalpy values, confirming the ability of PEG4000 in inducing the β-sheets conformation (Table 1).

In the ATR-FTIR spectra of cast materials prepared by blending the regenerated SF and the selected synthetic polymers, namely PEO, PVP, PEG 1000 and PEG4000 in the ratio 95/5% (w/w) SF molecules formed an ordered structure in the composite materials independently of the polymer blends since the main bands attributed to the amides stretching vibration overlapped with those of the degummed SF (Fig. 7). DSC data of the different SF/polymer blends obtained by casting revealed a single endothermic transition at about 297 °C attributed to thermal decomposition of SF (Hu et al., 2006), while the events due to the glass transition temperature at about 180 °C and the exothermic conversion from amorphous to crystalline at about 220 °C were not detected (Fig. 8). On the basis of these findings, it can be assumed that the contemporary use of blending with the selected hydrophilic polymers at the ratio of 95/5%, w/w and the casting procedure promotes the transition of SF to the β-sheet conformation.

Since PEG4000 was able to favour the β-sheet conformation of SF in the spray-dried material, it was considered worthily of investigation to study the effects of the PEG average molecular weights and PEG/SF ratios on the secondary structure of SF in cast materials. Four series were obtained by blending fibroin to PEG600, PEG1000, PEG1500 or PEG4000 and amide I of ATR-FTIR spectra were deconvoluted ($r^2 > 0.96$).

Fig. 9 shows the relative amounts of the secondary structural elements as function of SF/PEGs ratio. The contributions in presence of PEG4000 were not quantitatively reported because no reproducible data were obtained after casting the SF/PEG4000 blends at ratios higher than 95/5% (w/w). Indeed, the spectra recorded in different points of the cast materials did not overlap and the intensity of signals due to PEG4000 became more or less evident. The lack of miscibility in SF/PEG4000 cast material was also easily detected upon visual inspection: the material, generally homogeneous and transparent, became opaque and in some spots peeling features were evident (Fig. 10).

The molecular conformation of SF in cast materials prepared by using SF/PEG600 and SF/PEG1000 at the ratio 99/1%, w/w, was superimposable to the materials prepared by using the SF alone in terms of the relative amount of the secondary structural elements (Fig. 9). At the same ratio, PEG1500 or PEG4000 (B = 31.6%, R + A = 33.2%, T = 21.9%, SC = 13.3%) caused a slight increase of fractions of the β-sheets as well as side chains.

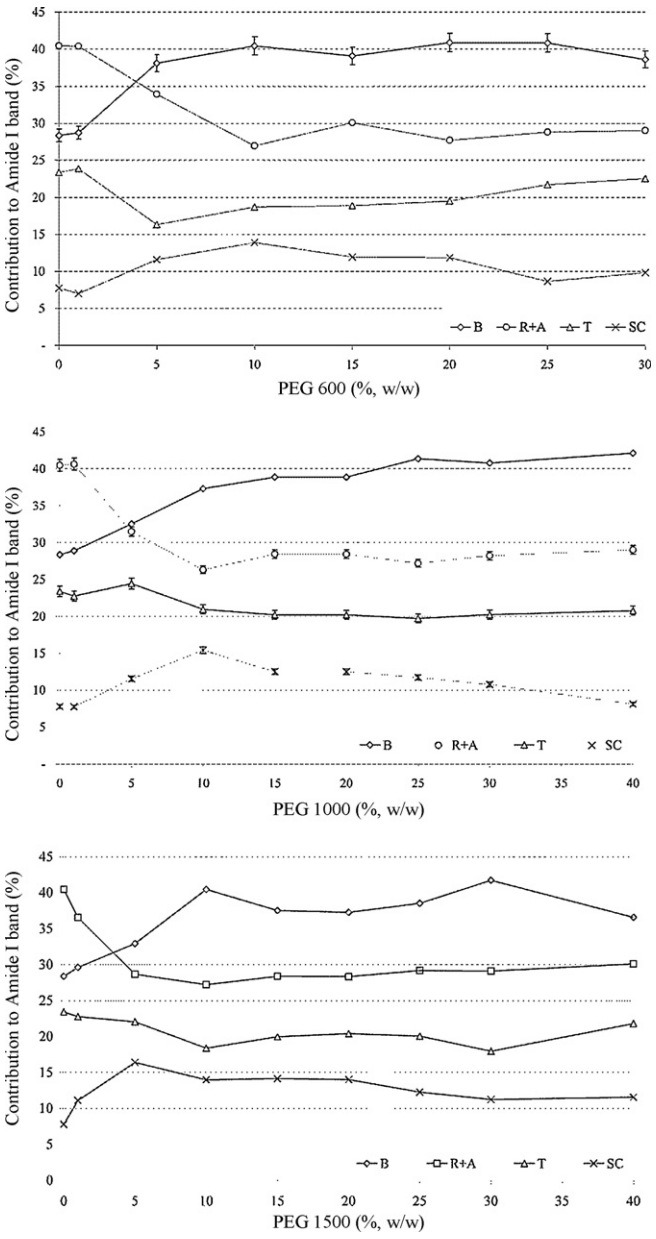

Fig. 9. Contributions to the ATF-FTIR amide I band determined by Fourier transform self-deconvolution for regenerated SF in cast materials as a function of the SF/PEG ratio and PEG molecular weight. Each data point represents the percentage of the peak areas attributed to: β-sheets (B); random coils and α-helices (R + A); turns (T); side chains (SC). The coefficient of variation of these data lower was than 3.5 ($n = 2$).

The higher the amount of blended PEG in the cast materials, the higher the contribution of the β-sheet fraction to the total amide I band area. Increasing of the PEG amount in the blends, the β-sheet fraction reached the constant value of about 40% removing differences in terms of molecular weight and ratio among series and reaching values of crystalline closer to that of the degummed fibroin (~50%). These finding were also in agreement with the DSC data. Indeed, when PEG600 was added to SF, the exothermic event recorded at about 206 °C was associated to a marked decrease in peak area (14 J/g). In addition, the higher crystallinity of the cast materials containing PEG4000 made the glass transition of the residual amorphous region less visible and more difficult to detect.

Fig. 10. Photography of a section of SF/PEG4000 film at the ratio 90/10% (w/w).

4. Conclusion

The amino acid composition (in mol%) of *B. mori* silk showed the predominance of five amino acids: Gly (42.9%), Ala (30.0%), Ser (12.2%), Tyr (4.8%), and Val (2.5%) (Zhou et al., 2000). The primary structure of *B. mori* silk fibroin may be approximately divided into four regions: (i) highly repetitive GAGAGS sequences constituting the crystalline region, (ii) relatively less repetitive GAGAGY and/or GAGAGVGY sequences comprising semicrystalline regions containing mainly hydrophobic moieties, (iii) sequences similar to (i) plus an extension by AAS, and (iv) amorphous regions containing negatively charged, polar, bulky hydrophobic, and aromatic residues (Zhou et al., 2000). The conformation of regenerated fibroin macromolecules and the transformation of their secondary structure are due to the rearrangement of the H-bonds especially in the (ii) regions. Even if these preliminary results should be deepened, it may be supposed that the tested synthetic polymers characterized by hydrogen acceptor groups, are able to form H-bonds with the tyrosine residues of SF which are largely located in the repetitive hexameric (–GAGAGY–) and octameric (–GAGAGVGY–) units of the semicrystalline regions (Zhou et al., 2000). This feature can favour the formation of an ordered structure of these regions during the evaporation process and, therefore, the transition from the typical conformation of regenerated SF, namely random coil, towards β-sheets. This interaction is probably influenced by the density and distribution of the H-bond acceptor groups in the polymer backbone. Indeed, while the tested polymers are able to induce the transition of the semicrystalline regions towards the stable conformation at slow evaporation rate, PEG 4000 was the only polymer able to promote a partial organization of SF in the stable form after spray drying.

Considering the homologous series of PEGs, higher the average molecular weight, i.e. the number of ether group for mass unit, higher the fraction of β-sheets as confirmed by the ATR-FTIR data of PEG4000/SF and PEG1000/SF spray dried products.

In conclusion, the approach to prepare SF/hydrophilic polymers composite materials at slow evaporation rate leads to water insoluble construct. These blends obtained by all-aqueous process technologies could be advantageously used to load drugs with instability issues in silk-based delivery systems avoiding final curing.

Acknowledgment

The Authors would like to thank Dr. G. Vistoli for the valuable discussions on molecular conformation of silk fibroin.

References

Boudet-Audet, M., Lefèvre, T., Buffeteau, T., Pézolet, M., 2008. Attenuated total reflection infrared spectroscopy: an efficient technique to quantitatively determine the orientation and conformation of proteins in single silk fibers. App. Spectrosc. 62, 956–962.

Cao, Y., Wang, B., 2009. Biodegradation of silk biomaterials. Int. J. Mol. Sci. 10, 1514–1524.

Hardy, J.G., Scheibel, T., 2010. Composite materials based on silk proteins. Prog. Pol. Sci. 35, 1093–1115.

Hino, T., Tanimoto, M., Shimabayashi, S.J., 2003. Change in secondary structure of silk fibroin during preparation of its microspheres by spray-drying and exposure to humid atmosphere. J. Colloid Interface Sci. 266, 68–73.

Hofmann, S., Wong Po Foo, C.T., Rossetti, F., Textor, M., Vunjak-Novakovic, G., Kaplan, D.L., Merkle, H.P., Meinel, L., 2006. Silk fibroin as an organic polymer for controlled drug delivery. J. Control. Release 111, 219–227.

Hu, X., Kaplan, D., Cebe, P., 2006. Determining beta-sheet crystallinity in fibrous protein by thermal analysis and infrared spectroscopy. Macromolecules 36, 6161–6170.

Kaplan, D.L., Mello, C.M., Arcidiacono, S., Fossey, S., Senecal, K., Muller, W., 1997. In: McGrath, K., Kaplan, D.L. (Eds.), Protein-based Materials. Birkhauser, Boston, pp. 103–131.

Kundu, J., Chung, Y.I., Kim, Y.H., Tae, G., Kundu, S.C., 2010. Silk fibroin nanoparticles for cellular uptake and control release. Int. J. Pharm. 388, 242–250.

Li, M., Lu, S., Wu, Z., Yan, H., Mo, J., Wang, L.J., 2001. Study on porous silk fibroin materials. I. Fine structure of freeze dried silk fibroin. Appl. Polym. Sci. 79, 2185–2191.

Minoura, N., Tsukada, M., Nagura, M., 2009. Physico-chemical properties of silk. Biomaterials 11, 430–434.

Numata, K., Kaplan, D.L., 2010. Silk-based delivery systems of bioactive molecules. Adv. Drug Del. Rev. 62, 1497–1508.

Sashina, E.S., Bochek, A.M., Novoselov, N.P., Kirichenko, D.A., 2006. Structure and solubility of natural silk fibroin. Russ. J. Appl. Chem. 79, 869–876.

Savitzky, A., Golay, J.E., 1964. Smoothing and differentiation of data by simplified least squares procedures. Anal. Chem. 36, 1628–1639.

Taddei, P., Monti, P., 2005. Vibrational Infrared conformational studies of model peptides representing the semicrystalline domains of *Bombyx mori* silk fibroin. Biopolymers 78, 249–258.

Vepari, C., Kaplan, D.L., 2007. Silk as a biomaterial. Prog. Polym. Sci. 32, 991–1007.

Wang, S., Wang, Q.H., Yang, X.L., Wang, L.Y., Zhu, H.S., 2003. Properties of silk fibroin/poly(ethylene glycol)400 blend films. Chin. J. Pol. Sci. 21, 87–91.

Wang, X., Wenk, E., Matsumoto, A., Meinel, L., Li, C., Kaplan, D., 2007. Silk microspheres for encapsulation and controlled release. J. Control. Release 117, 360–370.

Wang, X., Zhang, X., Castellot, J., Herman, I., Iafrati, M., Kaplan, D., 2008. Controlled release from multilayer silk biomaterial coatings to modulate vascular cell responses. Biomaterials 29, 894–903.

Zhou, C., Confalonieri, F., Medina, N., Zivanovic, Y., Esnault, C., Yang, T., Jacquet, M., Janin, J., Duguet, M., Perasso, R., Li, Z., 2000. Fine organization of *Bombyx mori* fibroin heavy chain gene. Nucleic Acids Res. 28, 2413–2419.